International Journal of
Neurooncology & Brain Tumors

Research Article

Radiomic Biomarkers Helps to Better Predict Progression Free Survival of Gliomas - ∂

Thibaut Kritter[1]*, Marco Rossi[2], Thierry Colin[1], Francois H Cornelis[3], Egesta Loci[2], Lorenzo Bello[2], Clair Poignard[1] and Olivier Saut[1]

[1]University of Bordeaux, IMB, UMR CNRS 5251 and INRIA Bordeaux-Sud-Ouest, Talence, France
[2]Neurosurgical Oncology Unit, Dept of Oncology and Hemato-Oncology, Universita degli Studi di Milano and Humanitas Research Hospital, IRCCS, Milan, Italy
[3]Sorbonne Universities, UPMC University Paris 06, APHP, HUEP, Tenon Hospital, Department of Radiology, 4 rue de la Chine, 75020 Paris, France

***Address for Correspondence:** T Kritter, University of Bordeaux, IMB, UMR CNRS 5251 and INRIA Bordeaux-Sud-Ouest, F-33400, Talence, France, E-mail: thibaut.kritter@inria.fr

Submitted: 12 December 2017; Approved: 26 December 2017; Published: 27 December 2017

Cite this article: Kritter T, Rossi M, Colin T, Cornelis FH, Loci E, et al. Radiomic Biomarkers Helps to Better Predict Progression Free Survival of Gliomas. Int J Neurooncol Brain Tumor. 2017;1(1): 014-020.

Copyright: © 2017 Kritter T, et al. This is an open access article distributed under the Creative Commons Attribution License, which permits unrestricted use, distribution, and reproduction in any medium, provided the original work is properly cited.

ABSTRACT

Purpose: To identify radiomic based biomarkers able to stratify on progression free survival patients presenting with gliomas.

Material and methods: Clinical, genetic and MR imaging features of 90 patients presenting lower grade gliomas (WHO grade II and III) were used in this study. An indicator of heterogeneity was identified accounting for spatial distribution of the tumor. Interesting features correlated with PFS were recorded and several machine learning strategies were compared to stratify patients into short or long PFS classes.

Results: MET-PET features appear to be strongly linked to PFS. Our method gives a good classification of fast or slow recurrence in 79% of the cases. This classification is more accurate than what is currently obtained with grade or IDH1 status and the combination of two.

Conclusion: Our method seems effective in patient's stratification to better predict clinical behavior. It constitutes a proof of concept of a tool which could have a role on the clinical evaluation of the risk of recurrence of gliomas.

INTRODUCTION

Gliomas account for 80% of primary malignant brain tumors [1,2]. They arise from glial cells and they are classified according to WHO classification of 2016, according to the presence of IDH1 mutation in 2 main categories: IDH1 wild type tumor represented mostly by grade IV Glioblastoma with very aggressive behavioral and poor prognosis – IDH1 mutated tumor that include various biological entities, graded according the same classification in grade II and III, with different biological behavior and prognosis. Recent publications, indeed, further reduce the value of histological grade as a prognostic factor.

The introduction of the new classification helps clinicians to better stratify patients and to tailor the best treatment according to tumor biology. Despite this new advances prognosis remains uncertain, particularly in the IDH1 mutated tumors.

The Progression-Free Survival (PFS) time is the duration between surgical treatment and clinical radiological recurrence of the disease. With a curative intend, surgery is thus often performed whatever the grade of tumors. However, the infiltrative nature of gliomas makes it difficult to obtain a complete resection at biological level [3]. Therefore, often additional treatments are used after the surgery to control the evolution, such as radiotherapy and chemotherapy. However as each of them carry risks of adverse effects, adequate treatments and adequate time for treatments have to be selected based on tumor's aggressiveness and patient's characteristics to improve oncological outcome and preserving quality of life of patients.

The European Association of Neuro-oncology recently published new guidelines for treatment of glioma in respect of the new classification, based on several RCT and on the clinical experience. The main feature driving the decision for treatment are – biology of the tumor and – risk group of the patient defined evaluating Karnofski Performance Status, neurological status and EOR. The introduction of this new guidelines suggest a substantial shared and homogeneous approach in the treatment of such a heterogeneous disease. The clinical problem is that despite a complex biological classification of the lesion and proper post-operative treatment, the clinical behavior remains unpredictable, suggesting that the actual molecular and clinical knowledge of this pathology is not powerful enough to efficiently stratify the patient in the clinical setting. Probably, one of the key point in this unsatisfying patient stratification using molecular features alone is the tumor heterogeneity, that fade away if the histological and molecular analysis in performed on small samples of tumor. Tumor heterogeneity can indeed be depicted with advance imaging study. Several published work suggest that radiological features and metabolic imaging, such as aminoacid PET, could help to predict, partially independently from biological features of the lesion, the aggressiveness of the tumor and clinical behavior after first line treatment. This results, still promising, are still far from optimum.

To better select patients requiring additional therapies and avoiding adverse effects in patients who don't need, a better selection based on tumor's aggressiveness and patient's characteristics is mandatory to improve the safety and quality of life of patients. To this end, the interest of radiomics-based analyses is highly increasing, in particular for brain tumors [4,5]. Thus far, such analysis has been performed using the grade of the tumor and the IDH1 status [6] However, the grade can sometimes be challenging to assess precisely, and behaviors among patients with the same grade or with the same IDH1 status can vary dramatically. The statistical analysis remained also limited on few imaging features without incorporation of 11C-methionine -PET scans [7] or biopsy information. MET-PET scans provide information about metabolic activities in different region of the tumor [8]. By using a patient-specific method and using all clinical genetic and imaging characteristics, our aim was to identify radiomic based biomarkers able to stratify on progression free survival patients presenting with gliomas.

MATERIALS AND METHODS

This retrospective study was approved by the institutional review board with patient informed consent and compliance with the Health Insurance Portability and Accountability Act. Patients agree to store their clinical information and materials in to the Humanitas Bio Bank, according to EC protocol 1299 Humanitas Research Hospital; each patient signed an informed consent. Humanitas Research Hospital Ethical Committee board approved this retrospective study. All methods were performed in accordance with relevant guidelines and regulations.

Patients

A total of 90 patients submitted to surgery and with a pathological diagnosis of lower grade glioma was included. Data were acquired and contains information from MRI, histological examination, MET-PET scan, clinical features and demographic information. All patient features are listed on table 1.

Neuroimaging protocol and EOR evaluation

In all patients a preoperative MR imaging was performed on a

Philips-Intera-3.0T, and acquired for lesion morphological and volumetric assessment. The MR protocol included: a) axial three-dimensional Fluid-Attenuated Inversion-Recovery (3D-FLAIR); b) post-gadolinium three-dimensional T1-weighted Fast-Field-Echo (FFE); c) DWI and ADC diffusion weighted imaging. Lesion volume was computed onto FLAIR volumetric sequences with manual segmentation using iPlanCranial software (BrainLabAG-Munich-Germany) by two investigators (M.R., L.B.). FLAIR hyperintense or T1W-gadolinium-enhanced signal abnormalities were included in the lesion load for LGGs or HGGs, respectively, and were reported in cm^3. Patients underwent both an immediate (within 48 h) and a 3-month postoperative MR scan (volumetric FLAIR and postGdT1-weighted images) to estimate the EOR. EOR corresponded to the percentage of the volume resected with respect to the pre-operative volume: (preoperative volume-postoperative volume)/ preoperative volume as previously published. Patients were then classified, according to EOR in partial (< 95%) or total resection (95-100% of EOR).

Metabolic Imaging

Detailed description of metabolic images acquisition was previously described by authors [9]. Briefly, all patient underwent ^{11}C-METH PET. The radiopharmaceutical used was carrier-free L-methyl-11C-methionine, synthesized in hospital. A mean activity of 300-500 MBq was administered and images were acquired 15 min later on a Biograph 6 LSO (Siemens Medical System) or a Discovery 690 GE PET/CT scanner. The acquired images were evaluated semiquantitatively. SUV ratio was calculated as the ratio between the count rate in Region of Interest (ROI) drawn on the area with the highest radiopharaceutical uptake (SUVmax) and a corresponding ROI drawn on the contralateral side. MTW was calculated as summed volume of voxels delineated on PET images.

Histological and Molecular Diagnosis

Samples obtained during surgery were analyzed in the pathology service of Humanities Research Hospital. IDH1 status was determined by immunohistochemistry and in case of negative expression by mutational analysis (codon132 of IDH1 gene, by DNA extraction -BiOstic FFPR rissue DNA isolation kit - and pyro sequencing of 132 codon, Diatech Pharmacogenetics IDH test). Codeletion was determined by FISH (probes: Vysis 1p36/1q25 e 19q13/19p13); ATRX loss, p53 mutation, Ki67 were determined by immunohistochemistry. For MGMT methylation status DNA was extracted (BiOstic FFPE Tissue DNA Isolation kit) and determined by pyrosequencing (Diatech Pharmacogenetics, MGMT plus, validated CE/IVD). Integrated diagnosis was used to classify tumors. Histological diagnosis revealed and were distributed like this: 43 grade II and 47 grade III (Figure 1). IDH1 mutation were present in 56 patients, IDH1 wild type in 25. In 48 cases the co-deletion 1p/19q were found. The MGMT metilation was found in 16 of the patients. For further details, see table 1.

Follow-up and post-operative treatment

All patients included in this study were followed in the post-operative period with clinical examination and periodic MR according to EANO indication [10]. According to the molecular classification and the risk group of the single patient, 60 patients received post-operative treatment (5 chemotherapy alone, 19 radiotherapy alone, 36 concomitant treatment).

All patients included in this study were discussed after surgery, in the neuro-oncology board and those patients who were selected for adjuvant treatment received chemotherapy or radiotherapy or concomitant treatment according to molecular and clinical features, as indicated in the last international guidelines. In particularly we defined high risk patient > 40 years old, who present neurological symptoms after surgery and with a partial resection. Chemotherapy and radiotherapy protocol are reported in table 1).We defined progression of disease, according to RANO criteria, by any of the following: (1) development of new lesions or increase of enhancement (radiological evidence of malignant transformation); (2) a 25% increase of the T2 or FLAIR non-enhancing lesion on stable or increasing doses of corticosteroids compared with baseline scan or best response after initiation of therapy, not attributable to radiation effect or to comorbid events; (3) definite clinical deterioration not attributable to other causes apart from the tumour, or decrease in corticosteroid dose; or (4) failure to return for evaluation because of death or deteriorating condition, unless caused by documented non-related disorders [11].

Demographics	age	44 years (17-81)
Clinical	lobe	31 frontal, 14 temporal, 10 parietal, 3 insula, 32 multiple
	cerebral hemisphere	44 left - 46 right
	first intervention	45 yes - 45 no
MRI	GD enhancing	25 yes- 65 no
	tumor volume	41.7 +/- 44.3 cm^3
Histomolecular diagnosis	grade	43 II - 47 III
	MIB1	8.2 +/- 9.2 %
	IDH1 status	56 mutated - 26 wild-type - 8 unknown
	1p expression	68 mutated - 6 wild-type - 16 unknown
	1q expression	49 mutated - 25 wild-type - 16 unknown
	codeletion	48 mutated - 26 wild-type - 16 unknown
	MGMT	61 yes - 13 no - 16 unknown
MET-PET	SUVmax	3.5 +/- 1.8
	SUVnorm	1.5 +/- 0.3
	SUVmean	2.3 +/- 1.1
	SUVratio (SUVmax/SUVnorm)	2.1 +/- 0.7
	MTV	13.3 +/- 17.0 cm^3
	MTB (SUVmean x MTV)	32.0 +/- 46.4 cm^3
Added data	Heterogeneity indicator	1.4 +/- 0.3
Follow-up	Extent of resection	54 total - 32 subtotal - 2 partial - 2 biopsy
	Recurrence	53 yes - 37 no
		grade II : 20 recurrent patients
		grade III : 33 recurrent patients
	Overall survival	32.8 +/- 12.9 months
	PFS	29.0 +/- 14.2 months
		grade II : 35 +/- 12 months
		grade III : 23 +/- 13 months
	Adjuvant Rx	60 yes - 30 no
	Lost in follow up	25 yes - 65 no

Table 1: Features of the database of 90 patients. The first part of the table contains features that are used for classification and the second part is the follow-up section. Grey tinted features are those which are quantitative, the others being qualitative. For quantitative values, the mean and the standard deviation are given.

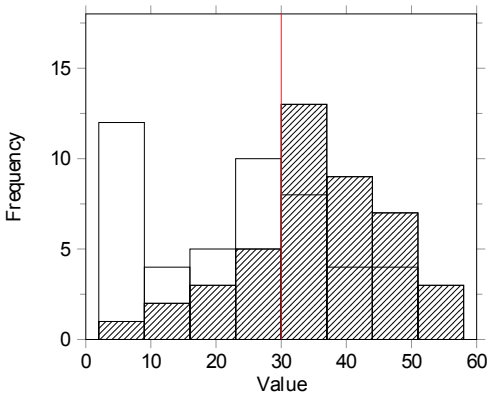

Figure 1: PFS histogram. PFS histogram of the database of 90 patients (in months). Plain blue bars represent grade 3 patients and dashed red bars represent grade 2 patients. The vertical line represents the threshold of 30 months. It separates fast (below 30 months) and slow (above 30 months) recurrence.

Outcomes

Recurrences were observed in 20 grade II and 33 grade III. Median PFS were 35 months (+/- 12 months) and 23 months (+/- 13 months), respectively. For the aim of this work a threshold has been arbitrary set at 30 months in order to separate slow progressing tumors from fast progressing ones. The rational of this threshold was for clinical reasons: it is commonly used in the clinical practice to guide eventual further treatment at tumor progression (second surgery, first or second line chemotherapy or radiotherapy). Our database contains 47 patients with slow recurrence and 43 patients with fast recurrence.

Features and heterogeneity criterion

Patient features are extracted from clinical, histological and radiological information. Extracted features from the MET-PET are the maximum and the mean of the SUV signal, the Metabolic Tumor Volume (MTV) and the Metabolic Tumor Burden (MTB).

To consider the signal heterogeneity, hotspots on the MET-PET scan were recorded by setting a threshold [12] on the signal and counting the number of connected component above this threshold. In order to account for spatial heterogeneity, a new indicator was set up. The idea is to count the number of connected components when the threshold varies in all the intensity range. This was done automatically for all the patients, by registrating the MET-PET scan on an atlas of a brain [13], focusing on the MET-PET signal inside the brain (Figure 2, left), setting the range of possible thresholds, and then calculating the number of connected components when the threshold varies. The minimal volume to detect a connected component was arbitrarily set to a cube of 3 voxel-long edge, to account for the noise on the image. For each patient, it gives a curve of the evolution of the number of spots, with respect to the threshold on the intensity. The given curves were integrated, in order to obtain an indicator: bigger the integral is, the more different spots there are in the tumor, and the more heterogeneous is the glioma. Other markers of heterogeneity were tried, such as the maximum of the calculated curve, or characteristic lengths calculated geometrically, but our new indicator is the most correlated to PFS (see Figure 3).

Feature selection

Our database contains more than 20 features for each patient, and these features are qualitative (histology, expression of genes) or quantitative (tumor volume, MET-PET information). In order to use classifier methods, one needs to focus only on the features which appear to be the most correlated to the PFS and the recurrence to the treatment. In order to figure out which features are the most relevant we use random forests technique [14]. Their advantage is to make appear the most important features of the data. The very few problems of missing data for histomolecular diagnosis was solved by imputing a constant distinct value instead. To further explore the ability of the method to classify patient and to evaluate the possibility to adopt the method as a pre-operative tool, we apply the same algorithm at the same cohort of patients without taking in to account the data available after surgery, such as Extent of Resection (EOR), histological diagnosis and grade, molecular features.

Factorial analysis of mixed data

In order to apply classification methods to the database, the reduction of the dimension of the space of features is necessary. Focusing on the important features previously obtained is a first step which has to be pushed forward. The idea is to use Principal

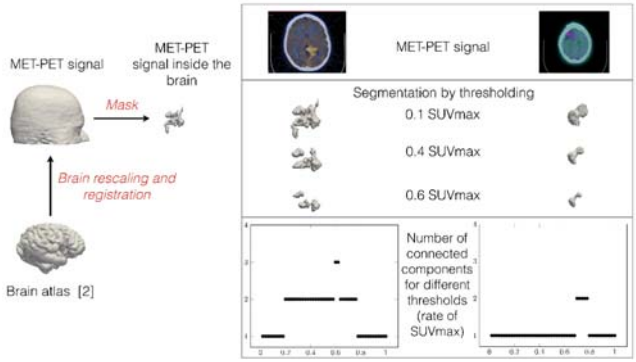

Figure 2: Heterogeneity indicator computation. Left: Registration of an atlas of a brain [14] to the MET-PET signal. Right: Two different behaviors of grade III tumors are compared. On the left column, the reconstructed MET-PET signal obtained with three different thresholds shows that there are one, two and then three different hotspots when the threshold grows (10, 40 and 60% of SUVmax). On the right column, the tumor is much more homogeneous, and the number of spots ranges from 1 to 2. The curves above (with 50 steps of SUVmax rate) give the total evolution of the number of spots when the threshold variates, and the integral of the left curve is bigger than the right one: the calculated indicator reports tumor heterogeneity on the MET-PET signal. PFS of left patient is under 30 months (9 months) whereas right patient has a slow recurrence (more than 33.6 months). It suggests that this indicator may impact the PFS classification, which is confirmed in the following section.

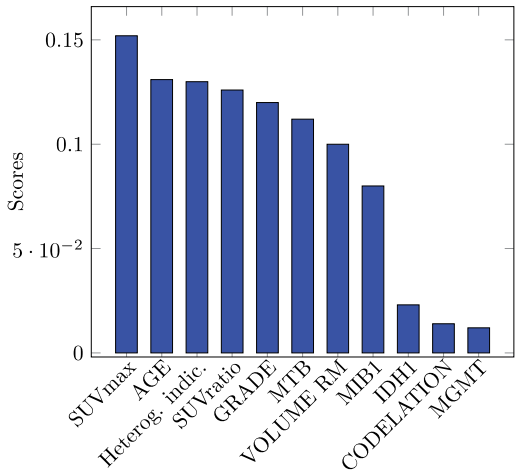

Figure 3: Correlated features to PFS. Scores of most important features regarding random forest classification of patients according to the PFS. Non represented features have a score lower than 0.01.

Component Analysis (PCA) and to project the original vectors on a well suited subspace. But PCA cannot be applied directly here because our database deals with qualitative and quantitative features (see Table 1). The idea is to use multivariate analysis of mixed data [15], in which PCA (for quantitative features) and Multiple Correspondence Analysis (MCA) (for qualitative ones) are combined. The data is preprocessed, and generalized singular value decomposition is then applied. This method also has the advantage of providing a new space of coordinates that are orthogonal to each other. Note that it can be useful in some classification methods to have non correlated variables (Bayes methods for example).

Machine learning methods and statistical analysis

Different classification methods were compared by using k -fold-cross-validation (with k = 10) [16]. Note that leave-one-out method

has also been tried and gives similar results. The following algorithms were compared: K-Nearest Neighbours (KNN), Naive Bayes Classifier, Logistic Regression, Random Forest, Multilayer Perceptron (MLP) and Support Vector Machines (SVM) [14]. The Python library Scikit-learn was used to implement these methods [17].

RESULTS

Feature selection

Feature selection by using random forests gives the histogram on figure 3. It shows a score of each feature regarding its usefulness for the stratification of our population of patients. Only the most relevant features are represented here and are kept in the database. Factorial analysis of mixed data is used to reduce the dimension of the space of characteristics. Machine learning methods are applied to the resulting subspace.

Machine learning analysis

The table 2 shows that all methods give pretty similar results, around 77 % of good classification. Interestingly, despite its simplicity, the k-nearest neighbours method minimizes the number of bad classifications (79% of good estimation), with a short computation time. On table 3, the table shows the number of well-predicted PFS in both categories. On figure 4, ROC (Receiver Operating Characteristic) curve [18] associated to the best classifier is plotted. The method applied without considering post-operative features (no histological diagnosis or grade, no IDH1 mutation) showed around 68% of good classification, and 70% by using Multilayer Perceptron method, as shown in table 4.

Classification comparison

On figure 5 panel A, three Kaplan-Meier curves [19] are compared. Both curves in blue dashed-line correspond to the survival curves of patients with grade II gliomas, and those with grade III gliomas. Red line curves are those obtained by dividing the same cohort of patients in two groups by using our classifier. Dotted lines represent IDH1 mutated and IDH1 wild type patients. Note that only 82 patients are classified by IDH1 as this information is missing for 8 patients. Our classifier separates the cohort even more significantly than the other ones. More precisely, log-rank statistic [20] of the grade classification and of the IDH1 mutation classification is much smaller than the one of the red line curves (X2_IDH1 = 7.8, X2_grade = 11.6 and X2_ML = 39.9). Cox regression [21] has also been used

Table 2: Six machine learning algorithms are compared by using k-fold cross validation (k = 10). The dataset is split into k folds. For each method, we run k different learning experiments with one of the fold as the testing set and the other folds as the training set. The final error of the method is the mean of the errors of the k learning experiments. The same splitting was made for each method to ensure a fair comparison.

Method	KNN	NaïveBayes	Logistic Reg	Random Forest	MLP	SVM
Error	0.211	0.233	0.244	0.267	0.244	0.233

Table 3: Classification by using k nearest neighbours method is the one that minimizes the number of misclassifications.

Real PFS PFS Prediction	Fast recurrence	Slow recurrence
Fast recurrence	33	9
Slow recurrence	10	38

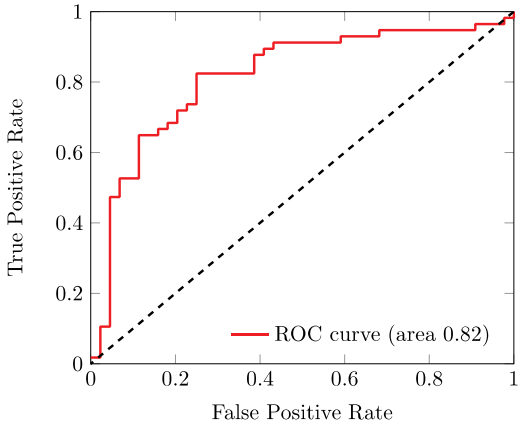

Figure 4: ROC curve. ROC curve associated to the best classifier, k nearest neighbours method. The area beyond the curve being above 0.8, the classifier is efficient.

to estimate Hazard Ratio (HR) in both cases. With our classification, HR = 5.59 (confidence interval 95%: 3.22-9.17), which means that the risk of recurrence at a given time t is on average 5.59 bigger for patients classified with fast recurrence than for those classified with slow recurrence. Classification by grade and by IDH1 mutation give smaller HR of 2.59 (CI 95%: 1.47-4.76) and 2.04 (CI 95%: 1.18-3.57) respectively.

The performance of our classifier were also compared white the classification of IDH1 and histological grade combined, as reported in figure 5 panel B. In B1 case, only grade II mutated and grade III wd patients are involved: our classifier and IDH1/grade combination give the exact same stratification, with a HR of 6.08 (CI 95%: 2.69-13.70). In B2 case, grade II wd and grade III mutated patients are kept which shows a much better stratification with our method (HR of 5.09 (CI 95%: 2.27-11.56) with ML, HR of 1.22 (0.38-1.73) with IDH1/grade separation).

The same workflow applied only to data acquired before surgery gives the resulting Kaplan-Meier curves on figure 5 panel C. The stratification of our classifier show a similar accuracy in patient stratification of the stratification according to grade and IDH1 mutation. In this case, HR is equal to 3.79 (CI 95%: 2.02-6.07), which is still bigger than HR of grade and IDH1 status.

DISCUSSION

Feature selection shows that, as expected, the age of the patient, the volume and the grade of the tumor are strongly correlated to PFS. IDH1 status (mutated or wild-type) and codeletion are supposed to be strongly linked to the aggressiveness of the tumor. The score of IDH1 status and codeletion is rather weak in our cohort. Missing information (for 8 and 16 patients respectively) may explain this weak score, as well as the fact that genomic information are local and may be less precise than MRI and PET-scans data which are global. Interestingly, the most correlated features are those measured on the MET-PET scan: SUV information, MTB and our indicator of heterogeneity are strongly linked to the prognosis of the patient. Actually, if active cells are heterogeneously spread out in the tumor, the surgery and the treatment may be less effective.

The percentage of good classifications is satisfactory, given that we only focus on biological features of the tumor and data acquired before the surgery and the treatment, and no longitudinal information

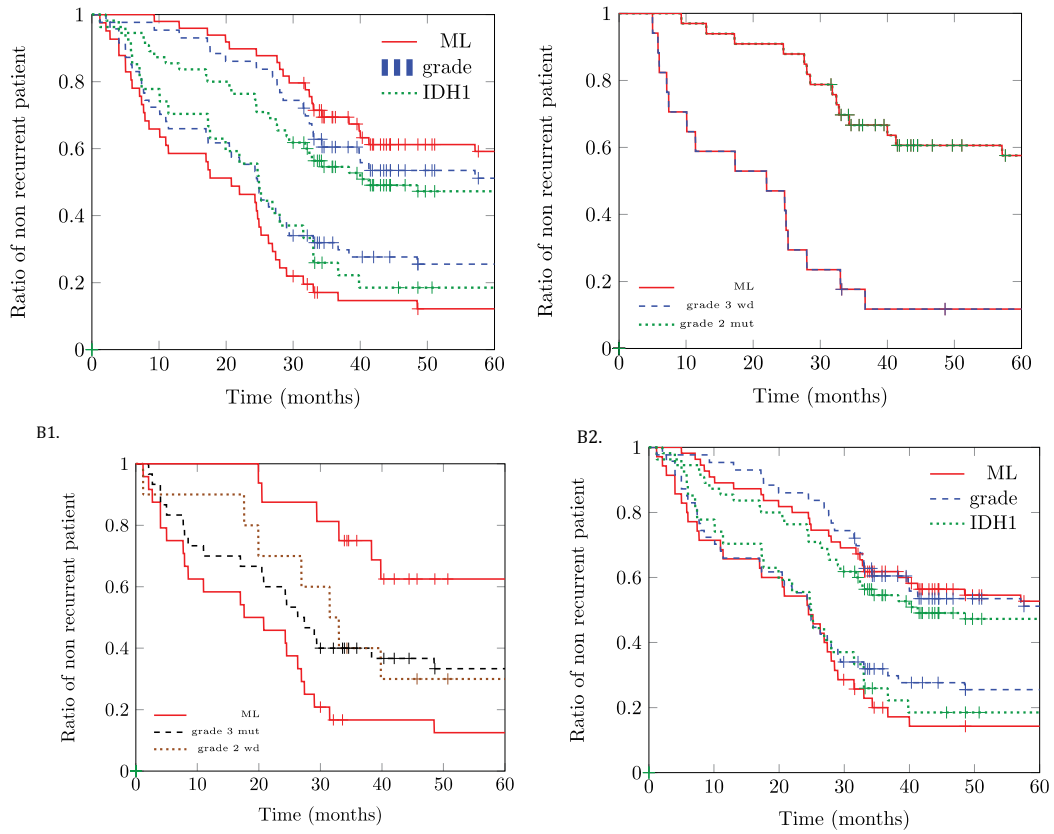

Figure 5: Kaplan Meier curves. A: Kaplan Meier curves for three different classifications: classified by low and high grade (blue dashed line), by IDH1 status (green dotted line, on 102 patients only) and by our best classifier (red solid line). B: Same Kaplan Meier curves but this time grade and IDH1 are combined: B1 curves focus only on grade II mutated and grade III wd patients, and B2 curves focus on grade II wd and grade III mutated patients. C: Same method, but only with data acquired before surgery (no grade, IDH1 and any biopsy or surgery information). Crosses represent patients with tumor which hasn't recurred yet.

has been used. The results are worse (74% of good classification) when the heterogeneity marker on MET-PET scans is not used, which suggests once again the relevance of this indicator. KNN method is the most efficient: this may be explained by the fact that there are many different clusters of patients that behave similarly, and other algorithms have more difficulties to catch these behaviors. Our algorithm stratifies patients more efficiently than what is currently used, such as grade, IDH1, and even the combination of the two, as shown by Hazard Ratio computation. In detail, as reported in figure 5 panel B1 , our classifier applied on grade II mutated and grade III wild type tumors gives the exact same stratification than what is obtained by separating grade II mutated and grade III wild type. But, as one can see in panel B2, our classifier stratifies much more efficiently grade II wd and grade III mutated patients, compared to classification by grade and IDH1 status. It is thus this population on which our method brings relevant information. Detecting fast recurrence more accurately can improve the follow-up of high-risk patients and help in type and timing of adjuvant treatment.

The same method applied without taking in account biological features of the tumor and EOR, showed a lower, but still satisfying accuracy in stratifying patients. The comparison of the method with the stratification according to biological features showed in fact similar PFS curves. For this reason, the method could be also further developed to be applied as a pre-operative tool to help clinicians in therapeutic decision and timing for surgery.

To summarize, the paper presents a method (Figure 6) combining preprocessing of the data, development of a novel heterogeneity marker that is computed automatically, and comparison of machine learning techniques in order to classify patients regarding their PFS. Combining the features extracted from different imaging modalities is a challenge that machine learning methods can overcome. In particular, it has shown that MET-PET scans features contain information correlated to the risk of recurrence, as well as our indicator of heterogeneity. Our method constitutes a proof of concept of a tool which could have a deep impact on the clinical evaluation of the risk of recurrence of gliomas when MET-PET imaging is available. Even if this availability of MET-PET imaging is quite limited, such method also works with any kind of modalities or clinical imaging, such as spectroscopy or diffusion. In particular, our indicator of heterogeneity can be computed on any images containing non homogeneous texture. Of course, such method needs to be validated on a bigger database, but the first results are promising.

ACKNOWLEDGEMENTS

This study has been carried out within the frame of the LABEX TRAIL, ANR-10-LABX-0057 with financial support from the French State, managed by the French National Research Agency (ANR) in the frame of the 'Investments for the future' Programme IdEx (ANR-10-IDEX-03-02).

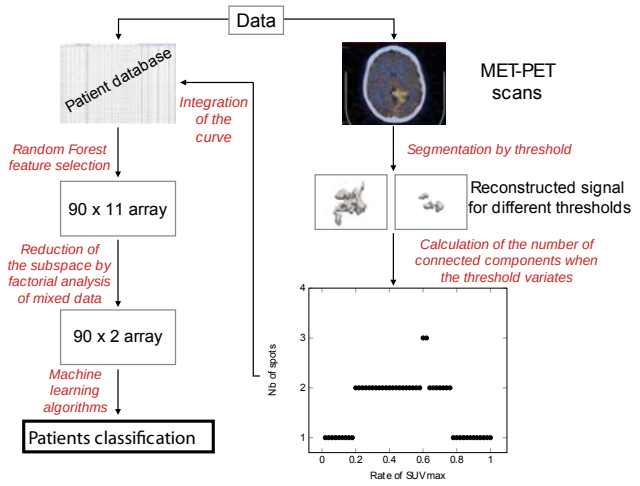

Figure 5: Workflow of the article. Description of the workflow used in the article. Right side explains the extraction of the indicator of heterogeneity from MET-PET scans. Left side shows the different steps from the database to the classification: feature selection, factorial analysis of mixed data and machine learning algorithms.

REFERENCES

1. Louis D N, Ohgaki H, Wiestler OD, Cavenee WK, Burger PC, Jouvet A, et al. The 2007 WHO Classification of Tumours of the Central Nervous System. Acta Neuropathol. 2007; 114: 97–109. https://goo.gl/eXMCGQ
2. Ostrom Q T. Gittleman H, Liao P, Rouse C, Chen Y, Dowling J, et al. CBTRUS Statistical Report: Primary Brain and Central Nervous System Tumors Diagnosed in theUnited States in 2007–2011. Neuro Oncol. 2014; 4: 1-63. https://goo.gl/1w8Ps5
3. Jakola AS. Myrmel KS, Kloster R, Torp SH, Lindal S, Unsgård G, Solheim O. Comparison of a Strategy Favoring Early Surgical Resection vs a Strategy Favoring Watchful Waitingin Low-Grade Gliomas. JAMA. 2012; 308: 1881-1888. https://goo.gl/NDppHc
4. Bourgier C J. Colinge N, Ailleres P, Fenoglietto M, Brengues A, Pelegrin, et al. Definition et applications cliniques des radiomics. Cancer/Radiotherapie. 2015 ; 19: 532 -537. https://goo.gl/TT4u64
5. Li Z, Wang Y, Yu J, Guo Y, Cao W. Deep learning based radiomics (dlr) and its usage in noninvasive idh1 prediction for low grade glioma. Sci Rep. 2017; 7: 5467. https://goo.gl/Gmpm5p
6. Louis DN. Perry A, Reifenberger G, von Deimling A, Figarella-Branger D, Cavenee WK, et al. The 2016 World Health Organization Classification of Tumors of the Central Nervous System: a summary. Acta Neuropathol. 2016; 131: 803-820. https://goo.gl/9rW18c
7. Glaudemans AW, Enting RH, Heesters MA, Dierckx RA, van Rheenen RW, Walenkamp AM, et al. Value of 11c-methionine pet in imaging brain tumours and metastases. Eur J Nucl Med Mol Imaging. 2013; 40: 615-635. https://goo.gl/Av4r2c
8. Zhu A, Lee D, Shim H. Metabolic PET Imaging in Cancer Detection and Therapy Response. Semin Oncol. 2011; 38: 55-69.https://goo.gl/cVMJhG
9. Lopci E, Riva M, Olivari L, Raneri F, Soffietti R, Piccardo A, et al. Prognostic value of molecular and imaging biomarkers in patients with supratentorial glioma. Eur J Nucl Med Mol Imaging. 2017; 44: 1155-1164. https://goo.gl/Na8cDu
10. Weller M. van den Bent M, Tonn JC, Stupp R, Preusser M, Cohen-Jonathan-Moyal E, Henriksson R, et al. European Association for Neuro-Oncology (EANO) guideline on the diagnosis and treatment of adult astrocytic and oligodendroglial gliomas. Lancet Oncol. 2017; 18: 315-329. https://goo.gl/1WH7Dz
11. van den Bent MJ. Wefel JS, Schiff D, Taphoorn MJ, Jaeckle K, Junck L, et al. Response assessment in neuro-oncology (a report of the RANO group): assessment of outcome in trials of diffuse low-grade gliomas. Lancet Oncol. 2011; 12: 583-593. https://goo.gl/tnywV5
12. Kim TM, Paeng JC, Chun IK, Keam B, Jeon YK, Lee SH, et al. Total lesion glycolysis in positron emission tomography is a better predictor of outcome than the International Prognostic Index for patients with diffuse large B cell lymphoma. Cancer. 2013; 119: 1195-1202. https://goo.gl/xfV3mU
13. Collins DL, AP Zijdenbos, V Kollokian. Design and construction of a realistic digital brain phantom. IEEE Transactions on Med. 1998; 17: 463-468. https://goo.gl/QoJzUw
14. Kotsiantis SB. Supervised Machine Learning: A Review of Classification Techniques. In Proceedings of the 2007 Conference on Emerging Artificial Intelligence Applications in Computer Engineering: Real Word AI Systems with Applications in eHealth, HCI, Information Retrieval and Pervasive Technologies, 2007; 3-24.
15. Chavent M, Kuentz-Simonet V, Labenne A, Saracco J. Multivariate analysis of mixed data: The PCAmixdata R package. arXiv. 2014 ; 1411-4911. https://goo.gl/L7KsNw
16. Kohavi, R. A study of cross-validation and bootstrap for accuracy estimation and model selection. In Proceedings of the 14th International Joint Conference on Artificial Intelligence.1995; 2: 1137–1143. https://goo.gl/bc7iRd
17. Pedregosa F. Gael Varoquaux, Alexandre Gramfort, Vincent Michel, Bertrand Thirion, Olivier Grisel, et al. Scikit-learn: Machine learning in Python. J Mach Learn Res. 2011; 12: 2825–2830. https://goo.gl/KhPbUb
18. Hajian-Tilaki K. Receiver Operating Characteristic (ROC) Curve Analysis for Medical Diagnostic Test Evaluation. Casp. Caspian J Intern Med. 2013; 4: 627-635. https://goo.gl/s7UvTU
19. Goel MK, Khanna P, Kishore J. Understanding survival analysis: Kaplan-Meier estimate. Int J Ayurveda Res. 2010; 1: 274-278. https://goo.gl/fT3hMG
20. Bland JM, Altman DG. The logrank test. BMJ. 2004; 328: 1073.
21. Spruance SL, Reid JE, Grace M, Samore M. Hazard Ratio in Clinical Trials. Antimicrob AgentsChemother. 2004; 48: 2787-2792. https://goo.gl/PE8MLe